

Gradient Statistics Aware Power Control for Over-the-Air Federated Learning in Fading Channels

Naifu Zhang and Meixia Tao

Abstract

To enable communication-efficient federated learning, fast model aggregation can be designed using over-the-air computation (AirComp). In order to implement a reliable and high-performance AirComp over fading channels, power control at edge devices is crucial. Existing works focus on the traditional data aggregation which often assumes that the local data collected at different devices are identically distributed and can be normalized with zero mean and unit variance. This assumption, however, does not hold for gradient aggregation in machine learning. In this paper, we study the optimal power control problem for efficient over-the-air FL by taking gradient statistics into account. Our goal is to minimize the model aggregation error measured by mean square error (MSE) by jointly optimizing the transmit power of each device and the denoising factor at the edge server. We first derive the optimal solution in closed form where the gradient first-order and second-order statistics are known. The derived optimal power control structure depends on multivariate coefficient of variation of gradient. We then propose a method to estimate the gradient statistics based on the historical aggregated gradients and then dynamically adjust the transmit power on devices over each training iteration. Experiment results show that our proposed power control is better than full power transmission and threshold-based power control in both model accuracy and convergence rate.

Index Terms

Federated learning, over-the-air computing, power control, fading channel.

I. INTRODUCTION

The proliferation of mobile devices such as smart mobile phones, wearable devices tablets has revolutionized people's daily lives. Due to the growing computation and sensing capabilities of

N. Zhang and M. Tao are with the Department of Electronic Engineering, Shanghai Jiao Tong University, Shanghai, 200240, P. R. China. (email: arthaslery@sjtu.edu.cn; mxtao@sjtu.edu.cn).

these devices, a wealth of data has been generated each day. This has promoted a wide range of artificial intelligence applications such as image recognition and natural language processing. Traditional machine learning procedure, including both training and inference, relies on cloud computing on a centralized data center with computing, storage, and full access to the entire data set. Wireless edge devices are thus required to transmit their collected data to a central parameter server, which can be very expensive in terms of energy and bandwidth consumption, as well as undesirable due to response delay and privacy concerns. It is thus increasingly desired to let edge devices engage in the learning process by keeping the collected data locally and performing training/inference either collaboratively or individually. This emerging technology is known as Edge Machine Learning [1].

Federated learning (FL) [2]–[4] is a new edge learning framework that enables many edge devices to collaboratively train a machine learning model without exchanging datasets under the coordination of an edge server in wireless networks. Compared with traditional learning at a centralized data center, FL offers several distinct advantages, such as preserving privacy, reducing network congestion, and leveraging distributed on-device computation. In FL, each edge device downloads a shared model from the edge server, computes an update to the current model by learning from its own local dataset, then sends this update to the edge server. Therein, the updates are averaged to improve the shared model.

The communication cost is the main bottleneck in FL since a large number of participating edge devices send their updates to the edge server at each round of the model training. Existing methods to obtain communication-efficient FL can be mainly divided into three categories, model parameter compression [5], [6], gradient sparsification [7], [8], and infrequent local update [2], [9]. Nevertheless, the communication cost of FL is still proportional to the number of edge devices, and thus inefficient in large-scale environment. Recently, a fast model aggregation approach is proposed for FL by applying over-the-air computation (AirComp) principle [10], such as in [11]–[14]. This is accomplished by exploring the waveform superposition nature of the wireless medium to compute the desired function of the distributed local gradient (i.e., the weighted average function) by concurrent transmission. Such AirComp-based FL, referred to as *over-the-air FL* in this work, can dramatically save the uplink communication bandwidth compared with existing approaches.

Due to the channel fading, device selection and power control are crucial to achieve a reliable

and high-performance over-the-air FL. In [15], the authors jointly optimize the transmit power at edge devices and the receive scaling factor (known as denoising factor) at the edge server. It is shown that the optimal power control in static channels exhibits a threshold-based structure. Namely, each device applies channel-inversion power control if its quality indicator exceeds the optimal threshold, and applies full power transmission otherwise. For AirComp-based gradient aggregation in FL, the work [12] introduces a truncation-based approach for excluding the edge devices with deep fading channels to strike a good balance between learning performance and aggregation error. The work [11] proposes a joint device selection and receiver beamforming design method to find the maximum selected devices with MSE requirements to improve the learning performance. These works [11], [12], [15] assume that the signal (i.e., the gradient) to be aggregated from each device is IID, and normalized with zero mean and unit variance. By exploiting the sparsity pattern in gradient vectors, the work [14] projects the gradient estimate in each device into a low-dimensional vector and transmits only the important gradient entries while accumulating the error from previous iterations. Therein, a channel-inversion like power control scheme, similar to those in [11], [12], [15] is designed so that the gradient vectors sent from selected devices are aligned at the edge server.

Note that all the existing works on power control for over-the-air FL have overlooked the following statistical characteristics of gradients. The gradient distribution over each iteration is independent but not necessarily identically distributed, and even in the same iteration, the distribution of each entry of the gradient vector can be non-identical. A general observation is that the gradient distribution changes over iterations and is different in each feature dimension. In addition, if the gradient distribution is unknown for each device, normalizing the gradient to a distribution with zero mean and unit variance is unrealistic. **Intuitively, the structure of optimal power control mainly depends on gradient statistics. Specifically, when gradient variance tends to zero, i.e., gradient of each device is the same, we should perform full power transmission for denoising and when gradient variance is large, we should perform channel-inversion transmission for reducing the variance.** As such, due to the neglect of gradient statistics, the existing power control methods for over-the-air FL would perform poorly in practice.

Motivated by the above issue, in this paper, we study the optimal power control problem for over-the-air FL over fading channels by taking gradient statistics into account. Our goal is to minimize the model aggregation error measured by MSE by jointly optimizing the transmit

power of each device and the denoising factor at the edge server given the first- and second-order statistics of gradients at each iteration. Through joint design, optimal power control minimizes aggregation errors in AirComp, and hence improves the convergence rate of FL. The main contributions of this work are outlined below:

- *Optimal power control with known gradient statistics:* We first derive the MSE expression of gradient aggregation at each iteration of the model training when the first-order and second-order statistics of the gradient vectors are known¹. We then formulate a joint optimization problem of transmit power at edge devices and denoising factor at the edge server for MSE minimization subject to individual peak power constraints at edge devices. By decomposing this non-convex problem into subproblems defined on different subregions, we obtain the optimal power control strategy in closed form. It is found that there is an optimal index threshold, below which the devices transmit with full power and above which the devices transmit at the power such that the equivalent weight of their gradients for aggregation are equalized.
- *Optimal power control in special case:* In two special cases of multivariate coefficient of variation of gradient tending to zero and infinity, the original problem is reduced to power independence between devices in optimization problem. In the first special case, the multivariate coefficient of variation of gradient tends to infinity. It is found that there is an optimal index threshold, below which the devices transmit with full power and above which the devices transmit at the power such that the equivalent weight of their gradients for aggregation are 1. Otherwise, it will perform a full power transmission. In the second special case, multivariate coefficient of variation of gradient tends to zero. It is found that the optimal power control is to let all the devices perform a full power transmission.
- *Adaptive power control with unknown gradient statistics:* We propose an adaptive power control algorithm that estimates the gradient statistics based on the historical aggregated gradients and then dynamically adjusts power values in each iteration. The communication cost consumed by estimating the gradient statistics are negligible compared to the transmission of the entire gradient vector.

¹Gradient statistics contains less information than gradient itself, thus known gradient statistics at edge server do not damage the privacy of local data.

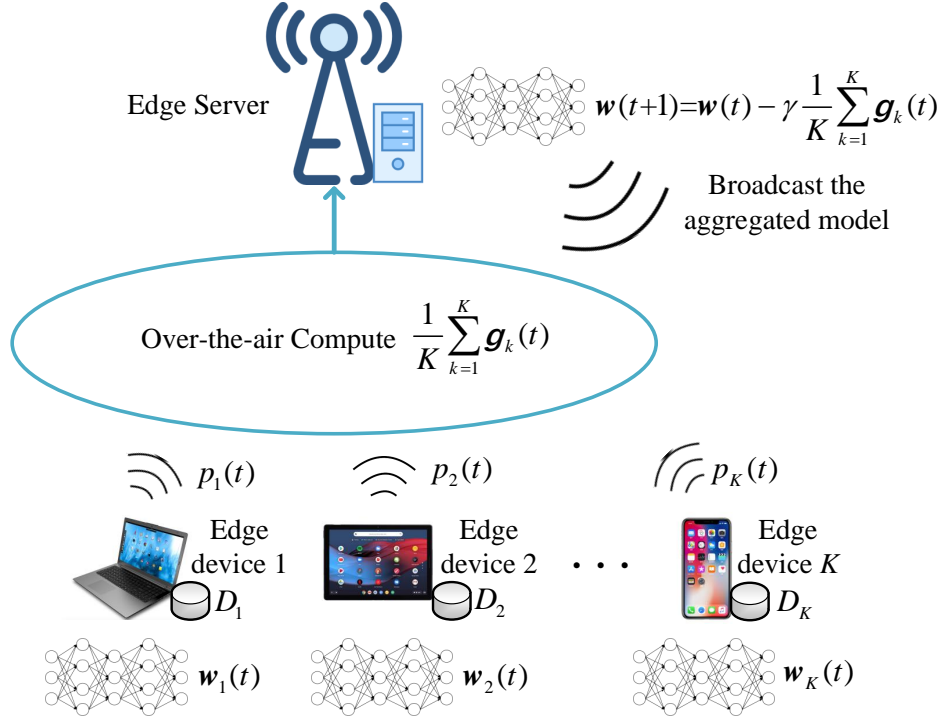


Fig. 1. Illustration of over-the-air federated learning.

The FL system is implemented in PyTorch for AI applications of three real image datasets. Experiment results show that the accuracy of over-the-air FL increases with the number of devices. We also observe that the over-the-air FL with the proposed adaptive power control obtains a much faster convergence rate than that with existing power control methods (full power transmission and threshold-based power control). Full power transmission performs bad in high SNR region and non-IID data distribution. Threshold-based power control performs bad in low SNR region and IID data distribution.

The rest of this paper is organized as follows. The fading channel FL system is modeled in the Section II, which presents power control problem for minimizing MSE. Section III describes the optimal power control strategy for two special cases and general case. In Section IV, an adaptive power control scheme for a general case is introduced. Finally, Section V provides experiment results and Section VI provides conclusions.

II. SYSTEM MODEL

A. Federated Learning Over Wireless Networks

We consider an FL setting over a wireless network where a shared AI model (e.g., a classifier) is trained collaboratively across K single-antenna edge devices via the coordination of a single-antenna edge server as shown in Fig. 1. Let $\mathcal{K} = \{1, \dots, K\}$ denote the set of edge devices. Each device $k \in \mathcal{K}$ collects a fraction of labelled training data via interaction with its own users, constituting a local dataset, denote as \mathcal{D}_k . The loss function measuring the model error is defined as

$$L(\mathbf{w}) = \sum_{k \in \mathcal{K}} \frac{|\mathcal{D}_k|}{|\mathcal{D}|} L_k(\mathbf{w}), \quad (1)$$

where $\mathbf{w} \in \mathbb{R}^D$ denotes the D -dimensional model parameter to be learned, $L_k(\mathbf{w}) = \frac{1}{|\mathcal{D}_k|} \sum_{i \in \mathcal{D}_k} l_i(\mathbf{w})$ is the loss function of device k quantifying the prediction error of the model \mathbf{w} on the local dataset collected at the k -th device, with $l_i(\mathbf{w})$ being the sample-wise loss function, and $\mathcal{D} = \bigcup_k \mathcal{D}_k$ is the global dataset. The minimization of $L(\mathbf{w})$ is typically carried out through stochastic gradient descent (SGD) algorithm, where device k 's local dataset \mathcal{D}_k is split into mini-batches of size B and at each iteration $t = 1, 2, \dots$, we draw one mini-batch $\mathcal{B}_k(t)$ randomly, and update the model parameter as

$$\mathbf{w}(t+1) = \mathbf{w}(t) - \gamma \frac{1}{K} \sum_{k \in \mathcal{K}} \nabla L_{k,t}^{SGD}(\mathbf{w}(t)), \quad (2)$$

with γ being the learning rate and $L_{k,t}^{SGD}(\mathbf{w}) = \frac{1}{B} \sum_{i \in \mathcal{B}_k(t)} l_i(\mathbf{w})$. The mean of the gradient $\nabla L_{k,t}^{SGD}(\mathbf{w}(t))$ in SGD is equal to the gradient $\nabla L(\mathbf{w}(t))$ in GD while the variance depends on the mini-batch size and distribution of data (IID or non-IID).

B. Over-The-Air Computation for Gradient Aggregation

We consider block fading channels, where the wireless channels remain unchanged within the duration of each iteration in FL but may change independently from one iteration to another. We define the duration of one iteration as one time block, indexed by $t \in \mathbb{N}$. It is assumed that the channel coefficients over different time blocks are generated from a stationary and ergodic process. Let $\mathbf{g}_k(t) \triangleq \nabla L_{k,t}^{SGD}(\mathbf{w}(t)) \in \mathbb{R}^D$ denote the gradient vector computed on device k at time block t . The following are key assumptions on the distribution of each entry, $g_{k,d}(t)$, of $\mathbf{g}_k(t)$:

- The gradient elements $\{g_{k,d}(t)\}, \forall k \in \mathcal{K}$, are independent and identically distributed over devices k 's. This is a default assumption since the distributions of the local datasets are unknown to the edge server and thus are treated equally².
- The gradient elements $\{g_{k,d}(t)\}, \forall t \in \mathbb{N}$, are independent but not identically distributed over iterations t 's. The non-identical distribution is valid since the gradient values in general change dynamically at the beginning, then gradually approach to zero as the training goes on.
- The gradient elements $\{g_{k,d}(t)\}, \forall d \in \{1, 2, \dots, D\}$, are independent but not identically distributed over gradient vector dimension d 's. This assumption is valid as long as the features in a data sample are independent but not identically distributed.

The gradient of interest at the edge server at time block t is given by

$$\mathbf{g}(t) = \frac{1}{K} \sum_{k \in \mathcal{K}} \mathbf{g}_k(t). \quad (3)$$

At each time block t , all the devices transmit their gradient vectors $\mathbf{g}_k(t)$ concurrently in an analog manner, following the AirComp principle. Each transmission block takes a duration of D slots, one slot for one entry in the D -dimensional gradient vector. Each gradient vector $\mathbf{g}_k(t)$ is multiplied with a pre-process factor, denoted as $b_k(t)$. The received signal vector at the edge server is given by

$$\mathbf{y}(t) = \sum_{k \in \mathcal{K}} b_k(t) h_k(t) \mathbf{g}_k(t) + \mathbf{n}(t), \quad (4)$$

where $h_k(t)$ denotes the channel coefficient from device k to the edge server³ and $\mathbf{n}(t)$ denotes the additive white Gaussian noise (AWGN) vector at the edge server with each element having zero mean and variance of σ_n^2 . To compensate the channel phase offset and control the actual transmit power at each device, we let $b_k(t) = \frac{\sqrt{p_k(t)} e^{-j\theta_k(t)}}{B_k(t)}$, where $p_k(t) \geq 0$ denotes the transmit power at device $k \in \mathcal{K}$ at each time block t , $\theta_k(t)$ is the phase of $h_k(t)$, and $B_k(t) \triangleq \|\mathbf{g}_k(t)\| = \sqrt{\sum_{d=1}^D g_{k,d}^2(t)}$ denotes the norm of the gradient $\mathbf{g}_k(t)$. Here, we have assumed that each device k can estimate perfectly the channel phase $\theta_k(t)$. By such design of $b_k(t)$, we can rewrite (4) as

$$\mathbf{y}(t) = \sum_{k \in \mathcal{K}} \frac{\sqrt{p_k(t)} |h_k(t)|}{B_k(t)} \mathbf{g}_k(t) + \mathbf{n}(t). \quad (5)$$

²The distribution of the gradients may be different when the local datasets are IID or Non-IID. However, the gradient elements are always independent and identically distributed across devices whether the local datasets are IID or Non-IID.

³We do not focus on channel estimation in this paper, thus channel coefficient is assumed to be known.

Each device $k \in \mathcal{K}$ has a peak power budget P_k , i.e.,

$$p_k(t) \leq P_k, \forall k \in \mathcal{K}, \forall t \in \mathbb{N}. \quad (6)$$

Upon receiving $\mathbf{y}(t)$, the edge server applies a denoising factor, denoted by $\eta(t)$, to recover the gradient of interest as

$$\hat{\mathbf{g}}(t) = \frac{\mathbf{y}(t)}{K\sqrt{\eta(t)}}, \quad (7)$$

where the factor $1/K$ is employed for the averaging purpose.

C. Performance Measure

We are interested in minimizing the distortion of the recovered gradient $\hat{\mathbf{g}}(t)$, with respect to (w.r.t.) the ground true gradient $\mathbf{g}(t)$. The distortion at a given iteration t is measured by the instantaneous MSE defined as

$$\begin{aligned} \text{MSE}(t) &= \mathbb{E}[\|\hat{\mathbf{g}}(t) - \mathbf{g}(t)\|^2] \\ &= \frac{1}{K^2} \mathbb{E} \left[\left\| \frac{\mathbf{y}(t)}{\sqrt{\eta(t)}} - \sum_{k \in \mathcal{K}} \mathbf{g}_k(t) \right\|^2 \right] \\ &= \frac{1}{K^2} \left[\sum_{d=1}^D \sigma_d^2(t) \sum_{k \in \mathcal{K}} \left(\frac{\sqrt{p_k(t)} |h_k(t)|}{\sqrt{\eta(t)} B_k(t)} - 1 \right)^2 \right. \\ &\quad \left. + \sum_{d=1}^D m_d^2(t) \left(\frac{1}{\sqrt{\eta(t)}} \sum_{k \in \mathcal{K}} \frac{\sqrt{p_k(t)} |h_k(t)|}{B_k(t)} - K \right)^2 + \frac{D\sigma_n^2}{\eta(t)} \right], \quad (8) \end{aligned}$$

where the expectation is over the distribution of the transmitted gradients $\mathbf{g}_k(t)$ and the received noise $\mathbf{n}(t)$. Note that the gradient norm $B_k(t)$ of each device k can be transmitted to the edge server with negligible communication cost, thus $B_k(t)$ is considered as a known value. In (8), $m_d(t)$ and $\sigma_d^2(t)$ denote the mean (first-order statistics) and variance (second-order statistics) of $g_d(t)$, the d -th entry of gradient $\mathbf{g}(t)$ at iteration t , respectively.

Our objective is to minimize MSE in (8), by jointly optimizing the transmit power $p_k(t)$ at devices and the denoising factor $\eta(t)$ at the edge server, subject to the individual peak transmit power constraints in (6).

D. Gradient Statistics

To facilitate the estimation of gradient statistics to be presented in Section IV, we introduce two alternative parameters. Let $\alpha(t)$ denote the mean squared norm (MSN) of $\mathbf{g}(t)$, i.e., $\mathbb{E}[\|\mathbf{g}(t)\|^2]$, which is given by

$$\alpha(t) = \sum_{d=1}^D \left(\sigma_d^2(t) + m_d^2(t) \right), \quad (9)$$

and let $\beta(t)$ denote the squared multivariate coefficient of variation (SMCV) of $\mathbf{g}(t)$, which is given by

$$\beta(t) = \frac{\sum_{d=1}^D \sigma_d^2(t)}{\sum_{d=1}^D m_d^2(t)}. \quad (10)$$

Figs. 2-4 illustrate the experiment results of the alternative gradient statistics $\alpha(t)$ and $\beta(t)$ of three different datasets, MNSIT, CIFAR-10, and SVHN, respectively, where the number of edge devices is 10 and the gradients are updated ideally without any transmission error. Both IID and non-IID distributions are considered for the training dataset. Each value of $\alpha(t)$ and $\beta(t)$ is obtained by averaging over 300 model trainings. It is seen that both the gradient MSN $\alpha(t)$ and the gradient SMCV $\beta(t)$ vary over iterations for all the three datasets. In particular, $\alpha(t)$ decreases over iterations and $\beta(t)$ increases over iterations. The former is due to the fact that the gradient amplitude gradually decreases when the model approaching convergence, while the latter is due to the fact that gradient mean decreases but gradient variance stays constant. It is also observed that the gradient SMCV $\beta(t)$ in non-IID distribution is much larger than that in IID distribution for all the three datasets. This is expected as the non IID distribution has divergent gradients on different devices. As such, we can conclude from Figs. 2-4 that the gradient statistics $\alpha(t)$ and $\beta(t)$ depend on both iterations and dataset distributions.

By (9) and (10), the MSE in (8) can be rewritten as, where we omit the constant coefficient $1/K^2$ for notational convenience.

$$\begin{aligned} \text{MSE}(t) = & \frac{\beta(t)\alpha(t)}{\beta(t)+1} \sum_{k \in \mathcal{K}} \left(\frac{\sqrt{p_k(t)}|h_k(t)|}{\sqrt{\eta(t)}B_k(t)} - 1 \right)^2 \\ & + \frac{\alpha(t)}{\beta(t)+1} \left(\frac{1}{\sqrt{\eta(t)}} \sum_{k \in \mathcal{K}} \frac{\sqrt{p_k(t)}|h_k(t)|}{B_k(t)} - K \right)^2 + \frac{D\sigma_n^2}{\eta(t)}. \end{aligned} \quad (11)$$

By observing (11) closely, we find that the MSE consists of three components, representing the individual signal misalignment error (the first term), the composite signal misalignment error (the

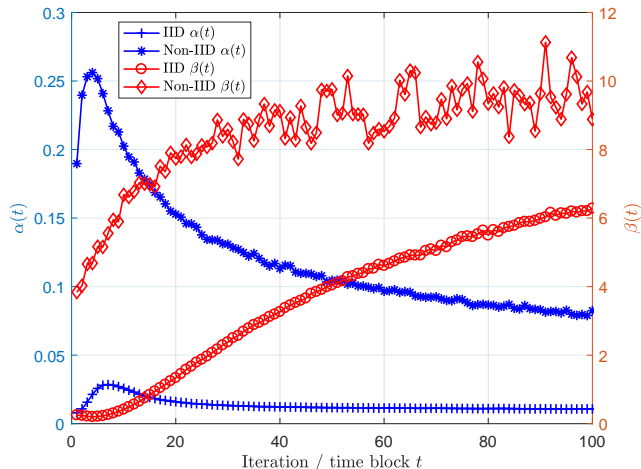


Fig. 2. Experiment results of MSN $\alpha(t)$ (left y-axis) and SMCV $\beta(t)$ (right y-axis) over iterations for dataset MNIST.

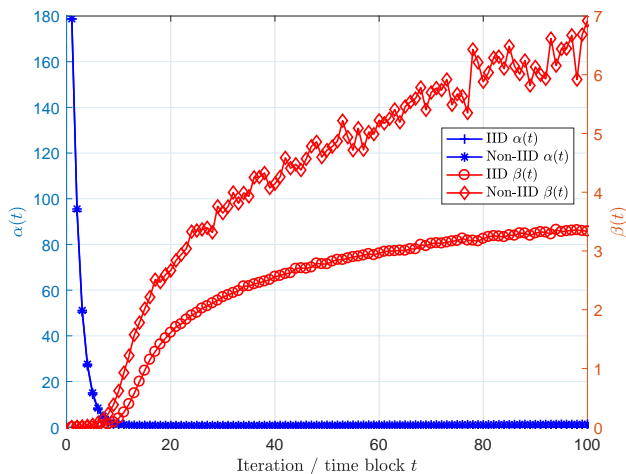


Fig. 3. Experiment results of MSN $\alpha(t)$ (left y-axis) and SMCV $\beta(t)$ (right y-axis) over iterations for dataset CIFAR-10.

second term), and the noise-induced error (the third term), respectively. In particular, the gradient SMCV $\beta(t)$ plays an important role. When $\beta(t) \rightarrow 0$, which can be the case when the model training just begins and/or the dataset distribution is IID, the individual signal misalignment error vanishes. When $\beta(t) \rightarrow \infty$, which can be the case when the model training converges and/or the dataset distribution is highly non-IID, the the composite signal misalignment error vanishes.

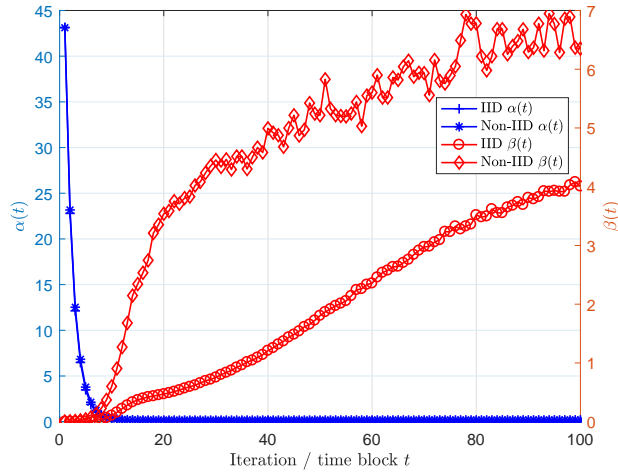


Fig. 4. Experiment results of MSN $\alpha(t)$ (left y-axis) and SMCV $\beta(t)$ (right y-axis) over iterations for dataset SVHN.

III. OPTIMAL POWER CONTROL WITH KNOWN GRADIENT STATISTICS

In this section, we formulate and solve the optimal power control problem for minimizing MSE when the gradient statistics $\alpha(t)$ and $\beta(t)$ are known. For convenience, we omit iteration index t in this section. For each device $k \in \mathcal{K}$, we also define its *gain level* with power p and denoising factor η as

$$G_k(p, \eta) = \frac{\sqrt{p}|h_k|}{\sqrt{\eta}B_k}, \quad (12)$$

which indicates the weight of the gradient from device k in the global gradient aggregation (7)⁴. Furthermore, we define *capability* of device k as its gain level with peak power P_k and unit denoising factor $\eta = 1$, i.e., $C_k = \frac{\sqrt{P_k}|h_k|}{B_k}$. Then we rank each device according to its capability as:

$$C_1 \leq \dots \leq C_k \leq \dots \leq C_K. \quad (13)$$

⁴The weight should be 1 for all devices in the ideal case.

A. Power Control Problem for General Case

In this subsection, we solve the optimal power control problem in general case, i.e., $0 < \beta < \infty$. The optimal power control problem of minimizing MSE is formulated as

$$\text{P1: } \min \frac{\beta\alpha}{\beta+1} \sum_{k \in \mathcal{K}} (G_k(p_k, \eta) - 1)^2 + \frac{\alpha}{\beta+1} \left(\sum_{k \in \mathcal{K}} G_k(p_k, \eta) - K \right)^2 + \frac{D\sigma_n^2}{\eta} \quad (14)$$

$$s.t. \quad 0 \leq p_k \leq P_k, \quad \forall k \in \mathcal{K} \quad (15)$$

$$\eta \geq 0. \quad (16)$$

Different from the power control problem in [15], the objective function in our P1 contains not only the individual misalignment error ($\frac{\beta\alpha}{\beta+1} \sum_{k \in \mathcal{K}} (G_k(p_k, \eta) - 1)^2$), but also the composite misalignment error ($\frac{\alpha}{\beta+1} (\sum_{k \in \mathcal{K}} G_k(p_k, \eta) - K)^2$) and the two errors cannot be minimized simultaneously. Problem P1 is non-convex in general. Even if the denoising factor η is given, problem P1 is still hard to solve due to the coupling of each power control p_k . In the following, we derive some properties of the optimal solution.

Lemma 1: Let η^* denote the optimal denoising factor for problem P1. It must satisfy $\eta^* \geq C_1^2$.

Proof: Please refer to Appendix A. ■

Lemma 1 reduces the range of denoising factor. Based on Lemma 1, we have the following lemma.

Lemma 2: The optimal power control policy satisfies $p_k^* = P_k, \forall k \in \{1, \dots, l\}, p_k^* < P_k, \forall k \in \{l+1, \dots, K\}$ for some $l \in \mathcal{K}$.

Proof: Please refer to Appendix B. ■

Lemma 2 shows that solving problem P1 is equivalent to minimizing the objective function in the following K subregions, denoted as $\{\mathcal{M}_l\}$, for $l = 1, \dots, K$, and comparing their corresponding optimal values to obtain the minimum one.

$$\mathcal{M}_l = \left\{ \mathbf{p} \in \mathbb{R}^K \mid p_k = P_k, \forall k \in \{1, \dots, l\}, 0 \leq p_k < P_k, \forall k \in \{l+1, \dots, K\} \right\}, \forall l \in \mathcal{K}. \quad (17)$$

To facilitate the derivation, we denote $\tilde{\mathcal{M}}_l$ as a relaxed version of \mathcal{M}_l by removing the condition $p_k < P_k$ for $k \in \{l+1, \dots, K\}$, which is given by

$$\tilde{\mathcal{M}}_l = \left\{ \mathbf{p} \in \mathbb{R}^K \mid p_k = P_k, \forall k \in \{1, \dots, l\}, p_k \geq 0, \forall k \in \{l+1, \dots, K\} \right\}, \forall l \in \mathcal{K}. \quad (18)$$

Taking the derivative of the objective function (14) w.r.t. p_k equating it to zero for all $k \in \{l+1, \dots, K\}$, we obtain the optimal power control $\tilde{p}_k(l)$ in the l -th relaxed subregion at any given η as

$$\tilde{p}_k(l) = \left[\frac{\beta + K - \sum_{i=1}^l G_i(P_i, \eta)}{\beta + K - l} \right]^2 \cdot \frac{B_k^2 \eta}{|h_k|^2}, k \in \{l+1, \dots, K\}. \quad (19)$$

Note that by such power control in (19) the gain level $G_k(\tilde{p}_k(l), \eta)$ of each device $k \in \{l+1, \dots, K\}$ is same. Substituting (19) back to (14), and letting the derivative of the objective function (14) w.r.t. η be zero, we can derive a closed-form optimal solution for denoising factor η in the l -th relaxed subregion, given by

$$\sqrt{\tilde{\eta}(l)} = \frac{\frac{\beta\alpha}{\beta+1} \sum_{k=1}^l C_k^2 + \frac{\beta\alpha}{(\beta+K-l)(\beta+1)} \left(\sum_{k=1}^l C_k \right)^2 + D\sigma_n^2}{\frac{\beta(\beta+K)\alpha}{(\beta+K-l)(\beta+1)} \sum_{k=1}^l C_k}. \quad (20)$$

Note that $\tilde{p}_k(l)$ may be not less than its power constraint P_k for some $k \in \{l+1, \dots, K\}$, and thus the corresponding $\tilde{\mathbf{p}}(l)$ does not lie in the subregion \mathcal{M}_l .

Lemma 3: For the problem defined in the l -th relaxed subregion $\tilde{\mathcal{M}}_l$, if $\exists k \in \{l+1, \dots, K\}, \tilde{p}_k(l) \geq P_k$, the optimal power \mathbf{p}^* of Problem P1 must not be in \mathcal{M}_l .

Proof: Please refer to Appendix C. ■

Lemma 3 shows that only the power control $\tilde{\mathbf{p}}(l)$'s with $\forall k \in \{l+1, \dots, K\}, p_k(l) < P_k$ are legal candidates of Problem P1. Let \mathcal{L} denote the index set of relaxed subregions with legal candidate power control. Note that \mathcal{L} is non-empty because $\tilde{\mathbf{p}}(K)$ is always a legal power control candidate. Then, we only need to compare the legal candidate values to obtain the minimum MSE:

$$l^* = \arg \min_{l \in \mathcal{L}} V_l, \quad (21)$$

where V_l is the optimal value of (14) in subregion \mathcal{M}_l . The optimal solution to problem P1 is derived as follows.

Theorem 1: The optimal transmit power at each device that solves problem P1 is given by

$$p_k^* = \begin{cases} P_k, & \forall k \in \{1, \dots, l^*\} \\ \left[\frac{\beta+K - \sum_{i=1}^{l^*} G_i(P_i, \eta^*)}{\beta+K-l^*} \right]^2 \cdot \frac{B_k^2 \eta^*}{|h_k|^2}, & \forall k \in \{l^*+1, \dots, K\}, \end{cases} \quad (22)$$

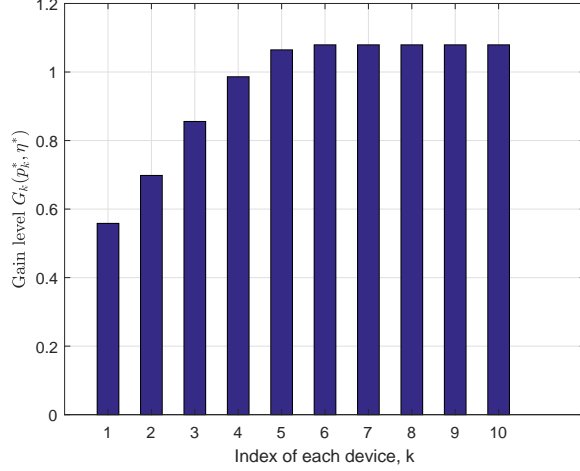


Fig. 5. Illustration of gain level with optimal power control.

and the optimal denoising factor at the edge server is given by

$$\sqrt{\eta^*} = \frac{\frac{\beta\alpha}{\beta+1} \sum_{k=1}^{l^*} C_k^2 + \frac{\beta\alpha}{(\beta+K-l^*)(\beta+1)} \left(\sum_{k=1}^{l^*} C_k \right)^2 + D\sigma_n^2}{\frac{\beta(\beta+K)\alpha}{(\beta+K-l^*)(\beta+1)} \sum_{k=1}^{l^*} C_k}, \quad (23)$$

where l^* is given in (21).

Proof: Please refer to Appendix D. ■

Remark 1: Theorem 1 shows that devices $k \in \{1, \dots, l^*\}$ with capability not higher than device l^* transmit their gradients with full power, i.e., $p_k = P_k$, while devices $k \in \{l^* + 1, \dots, K\}$ with capability higher than device l^* transmit gradients with the power so that they have the same gain level $G_k(p_k^*, \eta^*) = \frac{\beta+K-\sum_{i=1}^{l^*} G_i(P_i, \eta^*)}{\beta+K-l^*}$, somewhat analogous to channel inversion. Fig. 5 illustrates the gain level of all devices with the optimal power control in a system with $K = 10$ devices. The results are based on one channel realization of each device $|h_k|$ taken independently from normalized Rayleigh distribution. The peak power constraint of each device is set to be same with the average received SNR $= \frac{P_k}{D\sigma_n^2} = 0\text{dB}$. In this example, gradient norm of devices are $[0.23, 0.31, 0.26, 0.21, 0.30, 0.28, 0.22, 0.08, 0.28, 0.16]$, gradient MSN $\alpha = 0.06$, gradient SMCV $\beta = 5.5$ and $l^* = 5$. From Fig. 5 it is clearly seen that $G_k(p_k^*, \eta^*)$ is equal for $k = l^* + 1, \dots, K$.

Lemma 4: For $l \in \mathcal{K}$, the optimal power control $\tilde{p}(l)$ in the l -th relaxed subregion $\tilde{\mathcal{M}}_l$ satisfying $C_l \leq \frac{\sqrt{p_k(l)}|h_k|}{B_k} < C_{l+1}$, for $k = l + 1, \dots, K$, is equivalent to that $\tilde{p}(l)$ is the global optimal power control, i.e., $l^* = l$.

Proof: Please refer to Appendix E. ■

Lemma 4 shows that l^* remains unchanged over σ_n^2 and β as long as $\tilde{\mathbf{p}}(l^*)$ still satisfies $C_{l^*} \leq \frac{\sqrt{\tilde{p}_k(l^*)}|h_k|}{B_k} < C_{l^*+1}$, for $k = l^* + 1, \dots, K$. Thus the function \mathbf{p}^* of σ_n^2 and β is continuous in each subregion \mathcal{M}_{l^*} for $l^* = 1, \dots, K$. In order to prove that the optimal power control \mathbf{p}^* continuous globally with σ_n^2 and β , we have the following Lemma.

Lemma 5: The function \mathbf{p}^* of σ_n^2 and β continuous in each two adjacent subregions \mathcal{M}_l and \mathcal{M}_{l+1} for $l = 1, \dots, K - 1$.

Proof: Please refer to Appendix F. ■

Lemma 5 shows that if optimal power control is monotonic in each subregion, then optimal power control is monotonic globally. Based on (23) and (22), enlarging σ_n^2 increases η^* and enlarging η^* increases p_k^* for $k = l^* + 1, \dots, K$, thus, p_k^* monotonically increases with σ_n^2 . As the derivative of the objective function (22) w.r.t. β is always less than zero, thus p_k^* monotonically decreases with β . Furthermore, a larger σ_n^2 and a smaller β leads to more devices transmitting with full power, i.e., increasing the optimal l^* and vice versa.

B. Power Control Problem for Special Cases

In this subsection, we analyze the optimal power-control policy in two special cases, where gradient SMCV $\beta \rightarrow \infty$ and $\beta \rightarrow 0$, respectively.

1) $\beta \rightarrow \infty$: When $\beta \rightarrow \infty$, which could happen when the dataset distribution is non-IID and model approaches convergence. The optimal power control problem of minimizing MSE can be reformulated as

$$\text{P2: } \min \alpha \sum_{k \in \mathcal{K}} (G_k(p_k, \eta) - 1)^2 + \frac{D\sigma_n^2}{\eta} \quad (24)$$

$$\text{s.t. } 0 \leq p_k \leq P_k, \quad \forall k \in \mathcal{K} \quad (25)$$

$$\eta \geq 0. \quad (26)$$

Note that the problem P2 is consistent with the prior works in [15]. Thus, the threshold-based optimal power control proposed in [15] can be applied directly as follows.

Theorem 2: The optimal power control that solves problem P2 has a threshold-based structure, given by

$$p_k^* = \begin{cases} P_k, & \forall k \in \{1, \dots, l^*\} \\ \frac{B_k^2 \eta^*}{|h_k|^2}, & \forall k \in \{l^* + 1, \dots, K\}, \end{cases} \quad (27)$$

where the optimal denoising factor, also the threshold, is given as

$$\eta^* = \left(\frac{\alpha \sum_{k=1}^{l^*} C_k^2 + D\sigma_n^2}{\alpha \sum_{k=1}^{l^*} C_k} \right)^2, \quad (28)$$

and l^* is given in (21). Furthermore, it holds that $C_k^2 \leq \eta^*$ for devices $\forall k \in \{1, \dots, l^*\}$ and $C_k^2 \geq \eta^*$ for devices $\forall k \in \{l^* + 1, \dots, K\}$.

Proof: Please refer to [15, Theorem 1]. ■

Remark 2: Theorem 2 shows that when $\beta \rightarrow \infty$, devices $k \in \{1, \dots, l^*\}$ with capability not higher than $\sqrt{\eta^*}$ transmit gradients with full power, i.e., $p_k = P_k$, while devices $k \in \{l^* + 1, \dots, K\}$ with capability higher than $\sqrt{\eta^*}$ transmit gradient with same gain level 1. The optimal threshold η^* is a monotonically increasing function w.r.t. the noise variance σ_n^2 . In this special case, the denoising factor η^* is a threshold while it is not the threshold in general case.

2) $\beta \rightarrow 0$: When $\beta \rightarrow 0$, which could happen when the data distribution is IID and and the model training just starts, the power control problem of minimizing MSE can be reformulated as

$$\text{P3: } \min \quad \alpha \left(\sum_{k \in \mathcal{K}} G_k(p_k, \eta) - K \right)^2 + \frac{D\sigma_n^2}{\eta} \quad (29)$$

$$\text{s.t.} \quad 0 \leq p_k \leq P_k, \quad \forall k \in \mathcal{K} \quad (30)$$

$$\eta \geq 0. \quad (31)$$

It is observed that the objective function of problem P3 consists of the composite signal misalignment error and the noise-induced error.

First, we have the following lemma.

Lemma 6: The optimal denoising factor must satisfy

$$\eta^* \geq \frac{1}{K^2} \left(\sum_{k \in \mathcal{K}} C_k \right)^2. \quad (32)$$

Proof: Please refer to Appendix G. ■

The optimal solution to problem P3 is derived as follows.

Theorem 3: The optimal power control that solves problem P3 is full power transmission, given by

$$p_k^* = P_k, \quad \forall k \in \mathcal{K}, \quad (33)$$

and the optimal denoising factor that solves problem P3 is given by

$$\eta^* = \left(\frac{\alpha \left(\sum_{k \in \mathcal{K}} C_k \right)^2 + D\sigma_n^2}{\alpha K \sum_{k \in \mathcal{K}} C_k} \right)^2. \quad (34)$$

Proof: Please refer to Appendix H. ■

Remark 3: The optimal solution of problem P3 is the special case of the solution of problem P1 with $l^* = K$. Note that the direction of the gradient vector received from each device at the edge server is independent to the power of the transmitting device. Thus, increasing the power of all devices can reduce the noise-induced error when the composite signal misalignment error is fixed.

IV. ADAPTIVE POWER CONTROL WITH UNKNOWN GRADIENT STATISTICS

In this section, we consider practical scenarios where the gradient statistics $\alpha(t)$ and $\beta(t)$ are unknown. We propose a method to estimate $\alpha(t)$ and $\beta(t)$ in each time block. Then we propose an adaptive power control scheme based on the optimal solution of problem P1 using the estimated $\alpha(t)$ and $\beta(t)$.

A. Parameters Estimation

In this subsection, we propose a method to estimate $\alpha(t)$ and $\beta(t)$ at the at each time block t directly based on their definitions in (9) and (10), respectively.

1) *Estimation of $\alpha(t)$:* Since we assume that the instantaneous gradient norm of each device, $B_k(t)$, can be sent to the edge server with negligible cost, then by definition (9), we can estimate the gradient MSN as

$$\hat{\alpha}(t) = \frac{1}{K} \sum_{k \in \mathcal{K}} B_k^2(t). \quad (35)$$

2) *Estimation of $\beta(t)$:* By definition in (10), the gradient SMCV $\beta(t)$ depends on $m_d(t)$ and $\sigma_d(t)$. Knowing $m_d(t)$ is equivalent to recovering the gradient of interest in (7) at the edge server. Thus we cannot estimate $\beta(t)$ in advance before each device sending its gradient at time block t . Furthermore, Figs. 2-4 show that $\beta(t)$ changes slowly over iterations t . Thus we propose to estimate $\beta(t)$ based on the aggregated gradient at time block $t - 1$ as below:

$$\hat{\beta}(t) = \frac{\hat{\alpha}(t-1) - \sum_{d=1}^D \hat{g}_d^2(t-1)}{\sum_{d=1}^D \hat{g}_d^2(t-1)}, \quad (36)$$

where $\hat{\alpha}(t-1)$ estimates $\sum_d \sigma_d^2(t-1) + m_d^2(t-1)$ and $\sum_d \hat{g}_d^2(t-1)$ estimates $\sum_d m_d^2(t-1)$.

Algorithm 1 FL Process with Adaptive Power Control

- 1: Initialize $\mathbf{w}(0)$ in edge server, $\hat{\beta}(1)$;
 - 2: **for** time block $t = 1, \dots, T$ **do**
 - 3: Edge server broadcasts the global model $\mathbf{w}(t)$ to all edge devices $k \in \mathcal{K}$;
 - 4: **for** each device $k \in \mathcal{K}$ in parallel **do**
 - 5: $\mathbf{g}_k(t) = \nabla L_{k,t}^{SGD}(\mathbf{w}(t))$;
 - 6: $B_k(t) = \sqrt{\sum_d g_{k,d}^2(t)}$;
 - 7: Upload $B_k(t)$ to edge server;
 - 8: **end for**
 - 9: Edge server estimates $\hat{\alpha}(t)$ based on (35);
 - 10: Edge server obtains the optimal power control $\mathbf{p}^*(t)$ based on (22) and the optimal denoising factor $\eta^*(t)$ based on (23);
 - 11: Edge server sends $p_k^*(t)$ to device k for all $k \in \mathcal{K}$;
 - 12: **for** each device $k \in \mathcal{K}$ in parallel **do**
 - 13: Transmit gradient $\mathbf{g}_k(t)$ with power $p_k^*(t)$ to edge server using AirComp;
 - 14: **end for**
 - 15: Edge server receives $\mathbf{y}(t)$ and recovers $\hat{\mathbf{g}}(t)$ based on (7);
 - 16: Edge server estimates $\hat{\beta}(t+1)$ based on (36);
 - 17: Edge server updates global model $\mathbf{w}(t+1) = \mathbf{w}(t) - \gamma \hat{\mathbf{g}}(t)$;
 - 18: **end for**
 - 19: Edge server returns $\mathbf{w}(T+1)$;
-

B. FL with Adaptive Power Control

In this subsection, we propose the FL process with adaptive power control, which is presented in Algorithm 1. The algorithm has three steps. First, each device locally takes one step of SGD on the current model using its local dataset (line 5). After that each device calculates the norm of its local gradient and uploads it to the edge server with conventional digital transmission (line 7). Second, the edge server estimates parameters $\alpha(t)$ and $\beta(t)$ based on the received gradient norm at time block t and historical aggregated gradient (line 9 and line 16). Then the optimal power control and denoising factor are obtained based on (22) and (23), respectively (line 10). Third,

the edge server informs the optimal power control to each device and each device transmits local gradient with the assigned power simultaneously using AirComp to the edge server in an analog manner (line 12-14).

V. EXPERIMENT RESULTS

In this section, we provide experiment results to validate the performance of the proposed power control for AirComp-based FL over fading channels.

A. Experiment Setup

To evaluate the performance of our proposed adaptive power control algorithm, we conducted experiments on a simulated environment with the number of edge devices varying from 4 to 20. The wireless channels from each device to the edge server follow IID Rayleigh fading, such that h_k 's are modeled as IID complex Gaussian variables with zero mean and unit variance. For each device $k \in \mathcal{K}$, we define $\text{SNR}_k = \mathbb{E} \left[\frac{P_k |h_k|^2}{D\sigma_n^2} \right] = \frac{P_k}{D\sigma_n^2}$ as the average received SNR.

1) *Baselines*: We compare the proposed power control scheme with the following baseline approaches:

- *Error-free transmission*: the aggregated gradient is updated without any transmission error, which is equivalent to the centralized SGD algorithm.
- *Threshold-based power control in [15]*: this is the power control scheme given in [15], which assumed that signals are normalized. Note that it is actually the special case of our proposed power control scheme with $\beta = \infty$ by considering the individual mis-alignment error only in Problem P1.
- *Full power transmission*: all devices transmit with full power P_k and the edge server applies the optimal denoising factor in (23), where $l^* = K$.

2) *Datasets*: We evaluate the training of convolutional neural network on three different datasets, including MNIST, CIFAR10 and SVHN. MNIST dataset consists of 10 categories ranging from digit 0 to 9 and a total of 60000 labeled training data samples (50000 for training and 10000 for testing). CIFAR-10 dataset which includes 60000 color images (50000 for training and 10000 for testing) of 10 different types of objects. SVHN is a real-world image dataset for developing machine learning and object recognition algorithms with minimal requirement on

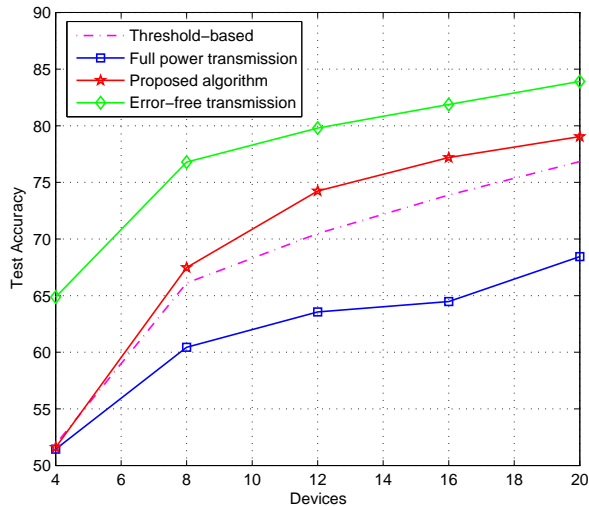


Fig. 6. Performance comparison over the number of devices, where MNIST dataset is non-IID distribution and the average received SNR of the K devices is set as 10 dB.

data preprocessing and formatting, which includes 60000 labeled training data samples (50000 for training and 10000 for testing).

3) *Data Distribution*: To study the impact of the SMCV of gradient β for power control, we simulate two types of data partitions among the mobile devices, i.e., the IID setting and non-IID one. For the former, we randomly partition the training samples into 100 equal shards, each of which is assigned to one particular device. While for the latter, we first sort the data by digit label, divide it into 200 shards of 300 images, and randomly assign 2 shards to each device.

4) *Training and Control Parameters*: In all our experiments, number of local update steps between two global aggregations is 1. Local batch size of each edge device is 10. The gradient descent step size is $\gamma = 0.01$.

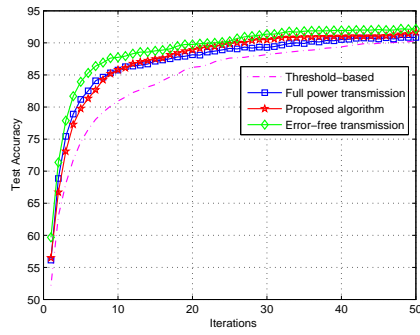
B. Experiment Results

1) *Varying Number of Devices*: The varying number of devices K is considered in Fig. 6, where MNIST dataset is non-IID distribution, the average received SNR of all the K devices is set as $\text{SNR}_k = 10\text{dB}$ and the results averaged over 50 channel realizations. Firstly, it is observed that the test accuracy achieved by all the three baselines increases as K increases, due to the fact that the edge server can aggregate more data for averaging and the equivalent SNR at the

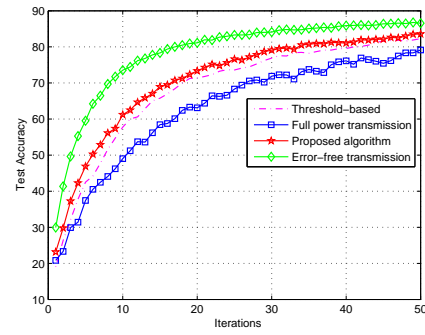
edge server is higher. Secondly, the proposed adaptive power control considerably outperforms both of threshold-based power control and full power transmission schemes throughout the whole regime of K . Full power transmission scheme approaches threshold-based power control scheme when K is small (i.e., $K = 4$ in Fig. 6), but the performance compromises as K increases, due to the lack of power adaptation to reduce the misalignment error.

2) *Varying gradient SMCV β* : The accuracy for datasets MNIST, CIFAR-10 and SVHN with IID dataset partition and non-IID dataset partition are shown in Fig. 7, respectively, where the average received SNR is set as 10dB and is equal for all devices with $K = 10$. It is observed that the achieved accuracy by all the four schemes increases over iterations, and the overall performance of the adaptive power control scheme is better than threshold-based power control scheme and full power transmission scheme. From Figs. 2-4, we know that the averaged gradient SMCV $\beta(t)$ in the IID partition is less than that in the non-IID partition and gradient SMCV $\beta(t)$ increases over iterations. The threshold-based power control scheme has significant accuracy loss compared to adaptive power control scheme in the IID partition or at the beginning of training. This is because in this case, the gradient SMCV is small and thus the MSE is dominated by the composite misalignment error. As a result, the threshold-based power control that considers the individual misalignment error only is much inferior. The full power transmission scheme has significant accuracy loss compared to adaptive power control scheme in the non-IID partition or at the end of training. This is because the gradient SMCV is large and therefore the full power transmission scheme fails to minimize the individual misalignment error that dominates the MSE in this case.

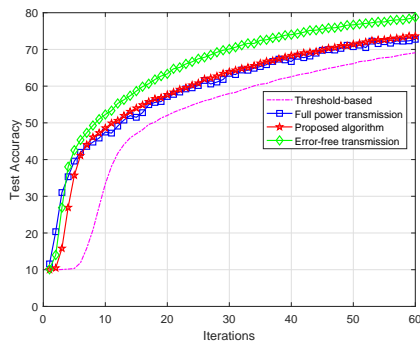
3) *Varying averaged SNR*: The test accuracy for MNIST is shown in Fig. 8 with the average received SNR set as 5dB and 10dB, respectively, where dataset is non-IID distribution and SNR is equal for all devices with $K = 10$. It is observed that the achieved accuracy by all the four schemes increases over iterations, and overall performance of the adaptive power control scheme is better than threshold-based power control and full power transmission schemes. The full power transmission scheme performs better than the threshold-based power control scheme when average received SNR is low. This is because that the full power transmission scheme can strongly suppress noise error, which is dominant for the MSE when average received SNR is low. The threshold-based power control scheme performs better than the full power transmission scheme when average received SNR is high. This is because that the threshold-based power control



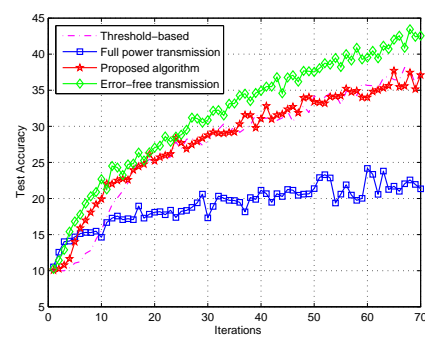
(a) Dataset MNIST IID.



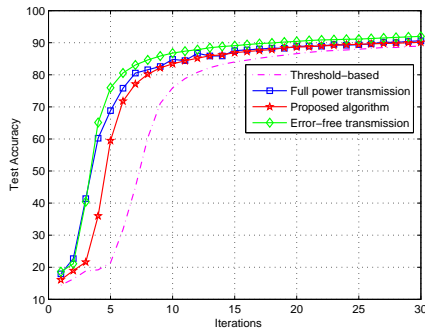
(b) Dataset MNIST non-IID.



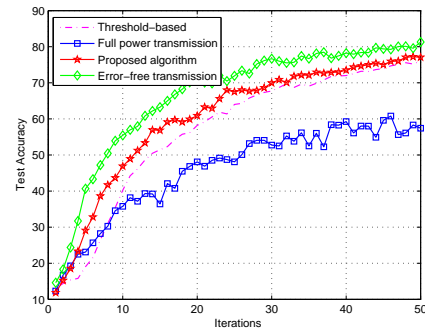
(c) Dataset CIFAR-10 IID.



(d) Dataset CIFAR-10 non-IID.



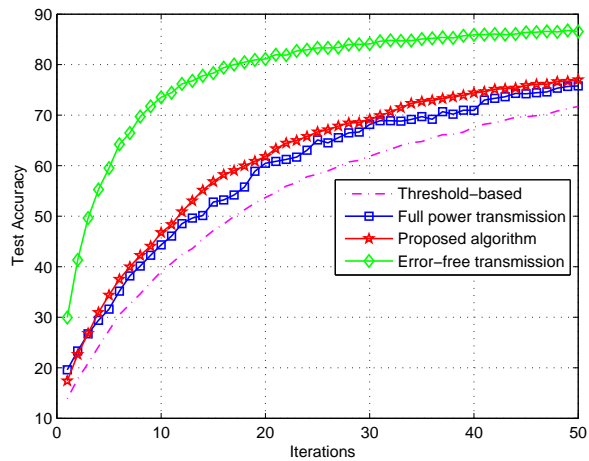
(e) Dataset SVHN IID.



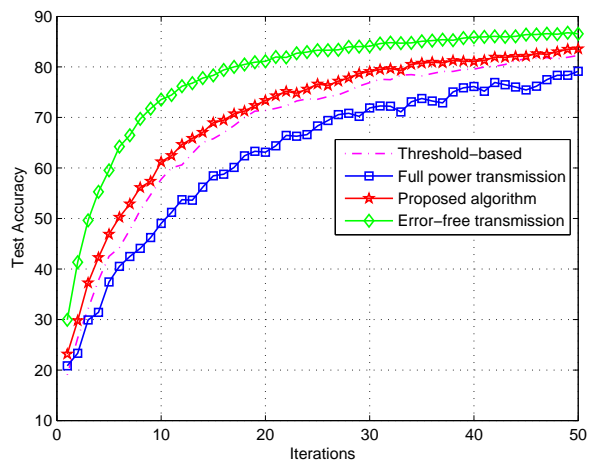
(f) Dataset SVHN non-IID.

Fig. 7. Performance comparison on different dataset partition, where number of edge devices is 10 and the average received SNR of the K devices is set as 10 dB.

scheme can suppress individual signal misalignment error while the full power transmission scheme ignores it, which is dominant for the MSE when average received SNR is high.



(a) Dataset MNIST 5dB.



(b) Dataset MNIST 10dB.

Fig. 8. Performance comparison on different average received SNR, where dataset is non-IID distribution MNIST, number of edge devices is 10.

VI. CONCLUSION

This work studied the power control optimization problem for the over-the-air federated learning over fading channels by taking the gradient statistics into account. The structure of the optimal power control for SGD learning mainly depends on the gradient SMCV β . When the gradient SMCV $\beta \rightarrow 0$, the optimal power control reduces to full power transmission. When the gradient SMCV $\beta \rightarrow \infty$, the optimal power control reduces to threshold-based power control.

The optimal power control monotonically increases with variance of noise σ^2 and monotonically decreases with the gradient SMCV β . We propose an adaptive power control scheme based on the estimated gradient SMCV $\hat{\alpha}$ and gradient MSN $\hat{\beta}$. Experiment results confirm that the accuracy of the over-the-air FL with our proposed adaptive power control outperforms the existing works. Full power transmission performs bad in high average received SNR region and non IID data distribution. Threshold-based power control performs bad in low average received SNR region and IID data distribution. Future work can investigate the optimal user schedule with asynchronous upload in digital manner. The key challenge lies in the number of sample calculated by devices can be a variable in each iteration due to the fact that a device can keep computing when other devices uploading parameters.

APPENDIX

A. Proof of Lemma 1

We prove this Lemma by contradiction. If the optimal denoising factor satisfies $\eta^* \leq C_1^2$, both the individual signal misalignment error $\frac{\beta\alpha}{\beta+1} \sum_{k \in \mathcal{K}} (G_k(p_k, \eta) - 1)^2$ and the composite signal misalignment error $\frac{\alpha}{\beta+1} (\sum_{k \in \mathcal{K}} (G_k(p_k, \eta) - K))^2$ can be minimized to zero by letting $p_k^* = \frac{\eta B_k^2}{|h_k|^2}, \forall k \in \mathcal{K}$. Therefore, the problem P1 can be expressed as

$$\min_{\eta} \frac{D\sigma_n^2}{C_1^2 \eta} \quad (37)$$

It is obvious that the optimal solution to this problem is $\eta^* = C_1^2$. As a result, it must hold that $\eta \geq C_1^2$ for problem P1.

B. Proof of Lemma 2

We prove this Lemma by contraction. Let $\mathbf{p}^* = [p_1^*, \dots, p_K^*]$ denote the optimal power control to the problem P1. We assume that there are two devices $k_1 < k_2$ satisfying $p_{k_1}^* < P_{k_1}$ and $p_{k_2}^* = P_{k_2}$. Let $\mathbf{p}' = [p_1^*, \dots, p_{k_1-1}^*, p'_{k_1}, p_{k_1+1}^*, \dots, p_{k_2-1}^*, p'_{k_2}, p_{k_2+1}^*, \dots, p_K^*]$ denote a modified power control, where $p'_{k_1} = P_{k_1}$ and p'_{k_2} satisfies $\frac{\sqrt{p_{k_1}^*} |h_{k_1}|}{\sqrt{\eta^*} B_{k_1}} + \frac{\sqrt{p_{k_2}^*} |h_{k_2}|}{\sqrt{\eta^*} B_{k_2}} = \frac{\sqrt{p'_{k_1}} |h_{k_1}|}{\sqrt{\eta^*} B_{k_1}} + \frac{\sqrt{p'_{k_2}} |h_{k_2}|}{\sqrt{\eta^*} B_{k_2}}$. The

difference between MSE of the power control \mathbf{p}^* and \mathbf{p}' is give by

$$\text{MSE}(\mathbf{p}^*) - \text{MSE}(\mathbf{p}') \quad (38)$$

$$= \frac{\beta\alpha}{\beta+1} \left[\left(\frac{\sqrt{p_{k_1}^*} |h_{k_1}|}{\sqrt{\eta^*} B_{k_1}} - 1 \right)^2 + \left(\frac{\sqrt{p_{k_2}^*} |h_{k_2}|}{\sqrt{\eta^*} B_{k_2}} - 1 \right)^2 - \left(\frac{\sqrt{p'_{k_1}} |h_{k_1}|}{\sqrt{\eta^*} B_{k_1}} - 1 \right)^2 - \left(\frac{\sqrt{p'_{k_2}} |h_{k_2}|}{\sqrt{\eta^*} B_{k_2}} - 1 \right)^2 \right] \quad (39)$$

$$= \frac{\beta\alpha}{\beta+1} \left[\left(\frac{\sqrt{p_{k_1}^*} |h_{k_1}|}{\sqrt{\eta^*} B_{k_1}} \right)^2 + \left(\frac{\sqrt{p_{k_2}^*} |h_{k_2}|}{\sqrt{\eta^*} B_{k_2}} \right)^2 - \left(\frac{\sqrt{p'_{k_1}} |h_{k_1}|}{\sqrt{\eta^*} B_{k_1}} \right)^2 - \left(\frac{\sqrt{p'_{k_2}} |h_{k_2}|}{\sqrt{\eta^*} B_{k_2}} \right)^2 \right] \quad (40)$$

$$= \frac{\beta\alpha}{\beta+1} \left(\frac{\sqrt{p_{k_2}^*} |h_{k_2}|}{\sqrt{\eta^*} B_{k_2}} - \frac{\sqrt{p'_{k_2}} |h_{k_2}|}{\sqrt{\eta^*} B_{k_2}} \right) \left(\frac{\sqrt{p_{k_2}^*} |h_{k_2}|}{\sqrt{\eta^*} B_{k_2}} + \frac{\sqrt{p'_{k_2}} |h_{k_2}|}{\sqrt{\eta^*} B_{k_2}} - \frac{\sqrt{p_{k_1}^*} |h_{k_1}|}{\sqrt{\eta^*} B_{k_1}} - \frac{\sqrt{p'_{k_1}} |h_{k_1}|}{\sqrt{\eta^*} B_{k_1}} \right) \quad (41)$$

$$= \frac{2\beta\alpha}{\beta+1} \left(\frac{\sqrt{p_{k_2}^*} |h_{k_2}|}{\sqrt{\eta^*} B_{k_2}} - \frac{\sqrt{p'_{k_2}} |h_{k_2}|}{\sqrt{\eta^*} B_{k_2}} \right) \left(\frac{\sqrt{p_{k_2}^*} |h_{k_2}|}{\sqrt{\eta^*} B_{k_2}} - \frac{\sqrt{p'_{k_1}} |h_{k_1}|}{\sqrt{\eta^*} B_{k_1}} \right) \quad (42)$$

$$> 0. \quad (43)$$

The inequality in (43) holds as $p_{k_2}^* = P_{k_2} > p'_{k_2}$ and $\frac{\sqrt{p_{k_2}^*} |h_{k_2}|}{\sqrt{\eta^*} B_{k_2}} > \frac{\sqrt{p'_{k_1}} |h_{k_1}|}{\sqrt{\eta^*} B_{k_1}}$. This indicates that \mathbf{p}^* is not the optimal power control, which contradicts the assumption. Therefore, for all pairs of two devices $k_1 < k_2$, if $p_{k_2}^* = P_{k_2}$, we must have $p_{k_1}^* = P_{k_1}$. Lemma 2 is thus proved.

C. Proof of Lemma 3

Assume that \mathbf{p}^* is in the l -th subregion \mathcal{M}_l , i.e., $\mathbf{p}^* \in \mathcal{M}_l$, and the optimal power control $\tilde{\mathbf{p}}(l)$ in the l -th relaxed subregion $\tilde{\mathcal{M}}_l$ is not in \mathcal{M}_l . The derivations of (19) and (23) show that $\tilde{\mathbf{p}}(l)$ is the only local optimal solution in the l -th relaxed subregion $\tilde{\mathcal{M}}_l$. As \mathbf{p}^* is the optimal power control in \mathcal{M}_l and cannot on the boundary of \mathcal{M}_l , then \mathbf{p}^* is also a local optimal solution in $\mathcal{M}_l \subseteq \tilde{\mathcal{M}}_l$. It contradicts that $\tilde{\mathbf{p}}(l)$ is the only local optimal solution in the l -th relaxed subregion $\tilde{\mathcal{M}}_l$. Therefore, if global optimal power control \mathbf{p}^* is in the l -th subregion \mathcal{M}_l , $\tilde{\mathbf{p}}(l)$ must be in \mathcal{M}_l . We complete the proof of Lemma 3.

D. Proof of Theorem 1

To complete the proof, we need to show that with l^* defined in (21), the optimal power control is the candidate power control \mathbf{p}^{l^*} . First, Lemma 1 and Lemma 2 tightens the range of optimal power to $\bigcup_{l \in \{1, \dots, K\}} \mathcal{M}_l$. Then Lemma 3 proved that the candidate power control not in \mathcal{L} cannot be the optimal power control and further tightens the range of optimal power to $\bigcup_{l \in \mathcal{L}} \mathcal{M}_l$. For all l in \mathcal{L} , the candidate power control is compliance with power constrain, thus the candidate power control \mathbf{p}^l is the optimal power control in the range \mathcal{M}_l . Therefore, the candidate power control \mathbf{p}^{l^*} with the smallest value V_{l^*} is the optimal power control of the problem P1. We complete the proof of Theorem 1.

E. Proof of Lemma 4

First we prove that the optimal power control \mathbf{p}^* holds $C_{l^*} \leq \frac{\sqrt{p_k^* |h_k|}}{B_k} < C_{l^*+1}$, for $k = l^* + 1, \dots, K$. As $p_k^* < P_k$ for $k = l^* + 1, \dots, K$, then $\frac{\sqrt{p_{l^*+1}^* |h_{l^*+1}|}}{B_{l^*+1}} < C_{l^*+1}$, thus we have the inequality in the right half $\frac{\sqrt{p_k^* |h_k|}}{B_k} < C_{l^*+1}$, for $k = l^* + 1, \dots, K$. We assume that $C_{l^*} > \frac{\sqrt{p_{l^*+1}^* |h_{l^*+1}|}}{B_{l^*+1}}$. As $\frac{p_k(l) |h_k|^2}{B_k} = C_k$ for all $k \in \{1, \dots, l^*\}$, $\frac{\sqrt{p_{l^*}^* |h_{l^*}|}}{B_{l^*}} = C_{l^*} > \frac{\sqrt{p_{l^*+1}^* |h_{l^*+1}|}}{B_{l^*+1}}$. Let $\mathbf{p}' = [p_1^*, \dots, p_{l^*}^*, p_{l^*+1}', \dots, p_K^*]$ denote a modified \mathbf{p}^* where power control $p_{l^*}^*$ and $p_{l^*+1}^*$ replaced by average of them, i.e., $\frac{\sqrt{p_{l^*}^* |h_{l^*}|}}{B_{l^*}} = \frac{\sqrt{p_{l^*+1}' |h_{l^*+1}|}}{B_{l^*+1}} = \frac{1}{2} \left(\frac{\sqrt{p_{l^*}^* |h_{l^*}|}}{B_{l^*}} + \frac{\sqrt{p_{l^*+1}^* |h_{l^*+1}|}}{B_{l^*+1}} \right)$. The difference between MSE of the power control \mathbf{p}^* and \mathbf{p}' is give by

$$\begin{aligned} & \text{MSE}(\mathbf{p}^*) - \text{MSE}(\mathbf{p}') \\ &= \frac{\beta\alpha}{\beta+1} \left[\left(\frac{\sqrt{p_{l^*}^* |h_{l^*}|}}{\sqrt{\eta^*} B_{l^*}} - 1 \right)^2 + \left(\frac{\sqrt{p_{l^*+1}^* |h_{l^*+1}|}}{\sqrt{\eta^*} B_{l^*+1}} - 1 \right)^2 \right. \\ & \quad \left. - \left(\frac{\sqrt{p_{l^*}^* |h_{l^*}|}}{\sqrt{\eta^*} B_{l^*}} - 1 \right)^2 - \left(\frac{\sqrt{p_{l^*+1}' |h_{l^*+1}|}}{\sqrt{\eta^*} B_{l^*+1}} - 1 \right)^2 \right] \end{aligned} \quad (44)$$

$$= \frac{\beta\alpha}{\beta+1} \left[\left(\frac{\sqrt{p_{l^*}^* |h_{l^*}|}}{\sqrt{\eta^*} B_{l^*}} \right)^2 + \left(\frac{\sqrt{p_{l^*+1}^* |h_{l^*+1}|}}{\sqrt{\eta^*} B_{l^*+1}} \right)^2 - \left(\frac{\sqrt{p_{l^*}^* |h_{l^*}|}}{\sqrt{\eta^*} B_{l^*}} \right)^2 - \left(\frac{\sqrt{p_{l^*+1}' |h_{l^*+1}|}}{\sqrt{\eta^*} B_{l^*+1}} \right)^2 \right] \quad (46)$$

$$= \frac{\beta\alpha}{2(\beta+1)} \left[\left(\frac{\sqrt{p_{l^*}^* |h_{l^*}|}}{\sqrt{\eta^*} B_{l^*}} - \frac{\sqrt{p_{l^*+1}^* |h_{l^*+1}|}}{\sqrt{\eta^*} B_{l^*+1}} \right)^2 \right] > 0. \quad (47)$$

The result indicates that \mathbf{p}^* is not the optimal power control, which contradicts the assumption. We have the inequality in the left half $C_{l^*} \leq \frac{\sqrt{p_k^* |h_k|}}{B_k}$. Thus, the necessity of this Lemma has been proved.

Second, we prove the inequality:

$$\frac{\sqrt{\tilde{p}_{l+1}(l) |h_{l+1}|}}{B_{l+1}} \geq C_{l+1}, \forall l \in \{1, \dots, l^* - 1\}. \quad (48)$$

We assume that $\exists l \in \{1, \dots, l^* - 1\}$, $\frac{\sqrt{\tilde{p}_{l+1}(l) |h_{l+1}|}}{B_{l+1}} < C_{l+1}$. As $\frac{\sqrt{\tilde{p}_k(l) |h_k|}}{B_k} = \frac{\sqrt{\tilde{p}_{l+1}(l) |h_{l+1}|}}{B_{l+1}}$ for all k in $\{l+1, \dots, K\}$ given in (19) and $C_{l+1} \leq C_k$ for all k in $\{l+1, \dots, K\}$ given in (13), then $\frac{\sqrt{\tilde{p}_k(l) |h_k|}}{B_k} < C_k$ for all k in $\{l+1, \dots, K\}$, thus $\tilde{\mathbf{p}}(l)$ is a feasible power control. Note that the constrain of optimizing the candidate power control $\tilde{\mathbf{p}}(l)$ is less restrictive than the constrain of optimizing the optimal power control \mathbf{p}^* . Thus, the feasible candidate power control $\tilde{\mathbf{p}}(l)$ is better than the optimal power control \mathbf{p}^* , which contradicts the assumption. We have the inequality (49).

Third, we prove the inequality:

$$\frac{\sqrt{\tilde{p}_{l+1}(l) |h_{l+1}|}}{B_{l+1}} < C_l, \forall l \in \{l^* + 1, \dots, K\}. \quad (49)$$

When $l = l^* + 1$, we assume that $\frac{\sqrt{\tilde{p}_{l+1}(l) |h_{l+1}|}}{B_{l+1}} \geq C_l$. Let $\mathbf{p}^{avg} = [\tilde{p}_1(l), \dots, \tilde{p}_{l-1}(l), p_l^{avg}, \dots, p_K^{avg}]$ denote a modified $\tilde{\mathbf{p}}(l)$, where $\tilde{p}_k(l)$ for $k = l, \dots, K$ replaced by average of them. Similar to (43), we can prove that $\text{MSE}(\mathbf{p}^{avg}) < \text{MSE}(\tilde{\mathbf{p}}(l))$. Let $\mathbf{p}^{fes} = [\tilde{p}_1(l), \dots, \tilde{p}_{l-1}(l), p_l^{fes}, \dots, p_K^{fes}]$ denote a modified $\tilde{\mathbf{p}}(l)$, where $\frac{\sqrt{p_k^{fes} |h_k|}}{B_k} = C_l$, for $k \in \{l, \dots, K\}$. The derivations of (19) and (23) show that enlarging η leads to a larger power control in l^* -th relaxed subregion $\tilde{\mathcal{M}}_{l^*}$ and a smaller MSE when $\eta \geq \tilde{\eta}(l^*)$. Note that \mathbf{p}^{avg} and \mathbf{p}^{fes} are in the l^* -th relaxed subregion $\tilde{\mathcal{M}}_{l^*}$ and $p_k^{avg} > p_k^{fes}$ for $k \in \{l, \dots, K\}$, thus $\text{MSE}(\mathbf{p}^{fes}) < \text{MSE}(\mathbf{p}^{avg}) < \text{MSE}(\tilde{\mathbf{p}}(l))$. The power control $\mathbf{p}^{fes} \in \tilde{\mathcal{M}}_l$ is better than the optimal power control $\tilde{\mathbf{p}}(l) \in \tilde{\mathcal{M}}_l$, which contradicts that $\tilde{\mathbf{p}}(l)$ is optimal solution in $\tilde{\mathcal{M}}_l$. We have the inequality (49).

For $l \in \mathcal{K}$, if $C_l \leq \frac{\sqrt{\tilde{p}_k(l) |h_k|}}{B_k} < C_{l+1}$, for $k = l+1, \dots, K$, then l cannot be in $\{1, \dots, l^* - 1\}$ or $\{l^* + 1, \dots, K\}$ based on (48) and (49), respectively. Therefore, $l = l^*$, i.e., $\tilde{\mathbf{p}}(l)$ is the global optimal power control. Thus, the adequacy of this Lemma has been proved.

We complete the proof of Lemma 4.

F. Proof of Lemma 5

Assume that the global optimal power control with $\sigma_n^2(l)$, $\alpha(l)$ and $\beta(l)$ lies in \mathcal{M}_l , which is denoted as $\mathbf{p}^*(l)$, and the corresponding denoising factor is denoted as $\eta^*(l)$. Assume that $\sigma_n^2(l) \rightarrow \sigma_n^2$, $\alpha(l) \rightarrow \alpha$ and $\beta(l) \rightarrow \beta$ so that $\frac{\sqrt{p_k^*(l)|h_k|}}{B_k} \rightarrow C_{l+1}$ for $k = l+1, \dots, K$. Based on (22), we have

$$\sqrt{\eta^*(l)} = \frac{\sum_{k=1}^l C_k + (\beta + K - l)C_{l+1}}{\beta + K}. \quad (50)$$

The global optimal power control with $\sigma_n^2(l+1) = \sigma_n^2$, $\alpha(l+1) = \alpha$ and $\beta(l+1) = \beta$ is denoted as $\mathbf{p}^*(l+1)$, and the corresponding denoising factor is denoted as $\eta^*(l+1)$. Based on (23) and (50) we have

$$\begin{aligned} & \frac{\frac{\beta\alpha}{\beta+1} \sum_{k=1}^l C_k^2 + \frac{\beta\alpha}{(\beta+K-l)(\beta+1)} \left(\sum_{k=1}^l C_k \right)^2 + D\sigma_n^2}{\frac{\beta(\beta+K)\alpha}{(\beta+K-l)(\beta+1)} \sum_{k=1}^l C_k} = \frac{\sum_{k=1}^l C_k + (\beta + K - l)C_{l+1}}{\beta + K} \\ \Leftrightarrow & \frac{\frac{\beta\alpha}{\beta+1} \sum_{k=1}^l C_k^2 + D\sigma_n^2}{\frac{\beta(\beta+K)\alpha}{(\beta+K-l)(\beta+1)} \sum_{k=1}^l C_k} = \frac{(\beta + K - l)C_{l+1}}{\beta + K} \\ \Leftrightarrow & \frac{\beta\alpha}{\beta + 1} \sum_{k=1}^l C_k^2 + D\sigma_n^2 = \frac{\beta\alpha}{\beta + 1} C_{l+1} \sum_{k=1}^l C_k \\ \Leftrightarrow & \frac{\beta\alpha}{\beta + 1} \sum_{k=1}^{l+1} C_k^2 + D\sigma_n^2 = \frac{\beta\alpha}{\beta + 1} C_{l+1} \sum_{k=1}^{l+1} C_k \\ \Leftrightarrow & \frac{\frac{\beta\alpha}{\beta+1} \sum_{k=1}^{l+1} C_k^2 + D\sigma_n^2}{\frac{\beta(\beta+K)\alpha}{(\beta+K-l-1)(\beta+1)} \sum_{k=1}^{l+1} C_k} = \frac{(\beta + K - l - 1)C_{l+1}}{\beta + K} \\ \Leftrightarrow & \frac{\frac{\beta\alpha}{\beta+1} \sum_{k=1}^{l+1} C_k^2 + \frac{\beta\alpha}{(\beta+K-l-1)(\beta+1)} \left(\sum_{k=1}^{l+1} C_k \right)^2 + D\sigma_n^2}{\frac{\beta(\beta+K)\alpha}{(\beta+K-l-1)(\beta+1)} \sum_{k=1}^{l+1} C_k} = \frac{\sum_{k=1}^{l+1} C_k + (\beta + K - l - 1)C_{l+1}}{\beta + K} \\ \Leftrightarrow & \sqrt{\eta^*(l+1)} = \sqrt{\eta^*(l)}, \end{aligned} \quad (51)$$

and based on (22) and (51), we have

$$\begin{aligned}
& \frac{\sqrt{\eta^*(l)}(\beta + K) - \sum_{k=1}^l C_k}{\beta + K - l} = C_{l+1} \\
& \Leftrightarrow \sqrt{\eta^*(l)}(\beta + K) - \sum_{k=1}^l C_k = (\beta + K - l)C_{l+1} \\
& \Leftrightarrow \sqrt{\eta^*(l+1)}(\beta + K) - \sum_{k=1}^{l+1} C_k = (\beta + K - l - 1)C_{l+1} \\
& \Leftrightarrow \frac{\sqrt{\eta^*(l+1)}(\beta + K) - \sum_{k=1}^{l+1} C_k}{\beta + K - l - 1} = C_{l+1} \\
& \Leftrightarrow p_k^*(l+1) = p_k^*(l), \forall k \in \{l+2, \dots, K\}, \tag{52}
\end{aligned}$$

and when $k = l + 1$, $p_k^*(l+1) = P_{l+1} = p_k^*(l)$. Therefore, the function \mathbf{p}^* and η^* of σ_n^2 , α and β continuous in \mathcal{M}_l and \mathcal{M}_{l+1} for $l = 1, \dots, K - 1$. We complete the proof of Lemma 5.

G. Proof of Lemma 6

Similar to the proof of Lemma 6, we prove this Lemma by contradiction. If the optimal denoising factor $\eta \leq \frac{1}{K^2} \left(\sum_{k \in \mathcal{K}} C_k \right)^2$, composite signal misalignment error $\left(\sum_{k \in \mathcal{K}} G_k(p_k, \eta) - K \right)^2$ can be minimized to zero. Therefore, the problem P3 can be expressed as

$$\min_{\eta \leq \frac{1}{K^2} \left(\sum_{k \in \mathcal{K}} C_k \right)^2} \frac{D\sigma_n^2}{\eta} \tag{53}$$

It is obvious that the optimal solution to this problem is $\eta^* = \frac{1}{K^2} \left(\sum_{k \in \mathcal{K}} C_k \right)^2$. As a result, it must hold that $\eta \geq \frac{1}{K^2} \left(\sum_{k \in \mathcal{K}} C_k \right)^2$ for problem P3. We complete the proof of Lemma 6.

H. Proof of Theorem 3

For any denoising factor $\eta \geq \frac{1}{K^2} \left(\sum_{k \in \mathcal{K}} C_k \right)^2$, it must hold that composite signal alignment $\sum_{k \in \mathcal{K}} G_k(p_k, \eta) \leq K$ for problem P3. Therefore, for minimizing composite signal misalignment error $\left(\sum_{k \in \mathcal{K}} G_k(p_k, \eta) - K \right)^2$, all the devices should always transmit with full power, i.e., $p_k^* = P_k, \forall k \in \mathcal{K}$. The problem P3 can be expressed as

$$\min_{\eta \geq 0} \alpha \left(\sum_{k \in \mathcal{K}} G_k(p_k, \eta) - K \right)^2 + \frac{D\sigma_n^2}{\eta} \tag{54}$$

This is a unary quadratic function about $\frac{1}{\sqrt{\eta}}$, thus it is easy to derive an optimal solution given by

$$\eta^* = \left(\frac{\alpha \left(\sum_{k \in \mathcal{K}} C_k \right)^2 + D\sigma_n^2}{\alpha K \sum_{k \in \mathcal{K}} C_k} \right)^2. \quad (55)$$

We complete the proof of Theorem 3.

REFERENCES

- [1] J. Park, S. Samarakoon, M. Bennis, and M. Debbah, “Wireless network intelligence at the edge,” *Proceedings of the IEEE*, vol. 107, no. 11, pp. 2204–2239, 2019.
- [2] H. B. McMahan, E. Moore, D. Ramage, S. Hampson *et al.*, “Communication-efficient learning of deep networks from decentralized data,” *arXiv preprint arXiv:1602.05629*, 2016.
- [3] K. Bonawitz, H. Eichner, W. Grieskamp, D. Huba, A. Ingerman, V. Ivanov, C. Kiddon, J. Konecny, S. Mazzocchi, H. B. McMahan *et al.*, “Towards federated learning at scale: System design,” *arXiv preprint arXiv:1902.01046*, 2019.
- [4] Q. Yang, Y. Liu, T. Chen, and Y. Tong, “Federated machine learning: Concept and applications,” *ACM Transactions on Intelligent Systems and Technology (TIST)*, vol. 10, no. 2, p. 12, 2019.
- [5] D. Alistarh, D. Grubic, J. Li, R. Tomioka, and M. Vojnovic, “Qsgd: Communication-efficient sgd via randomized quantization and encoding,” *Advances in Neural Information Processing Systems 30*, vol. 3, pp. 1710–1721, 2018.
- [6] F. Seide, H. Fu, J. Droppo, G. Li, and D. Yu, “1-bit stochastic gradient descent and its application to data-parallel distributed training of speech dnns,” in *Fifteenth Annual Conference of the International Speech Communication Association*, 2014.
- [7] A. F. Aji and K. Heafield, “Sparse communication for distributed gradient descent,” *arXiv preprint arXiv:1704.05021*, 2017.
- [8] Y. Tsuzuku, H. Imachi, and T. Akiba, “Variance-based gradient compression for efficient distributed deep learning,” *arXiv preprint arXiv:1802.06058*, 2018.
- [9] S. Wang, T. Tuor, T. Salonidis, K. K. Leung, C. Makaya, T. He, and K. Chan, “Adaptive federated learning in resource constrained edge computing systems,” *IEEE Journal on Selected Areas in Communications*, vol. 37, no. 6, pp. 1205–1221, 2019.
- [10] B. Nazer and M. Gastpar, “Computation over multiple-access channels,” *IEEE Transactions on information theory*, vol. 53, no. 10, pp. 3498–3516, 2007.
- [11] K. Yang, T. Jiang, Y. Shi, and Z. Ding, “Federated learning via over-the-air computation,” *arXiv preprint arXiv:1812.11750*, 2018.
- [12] G. Zhu, Y. Wang, and K. Huang, “Low-latency broadband analog aggregation for federated edge learning,” *arXiv preprint arXiv:1812.11494*, 2018.
- [13] M. M. Amiri and D. Gündüz, “Machine learning at the wireless edge: Distributed stochastic gradient descent over-the-air,” in *2019 IEEE International Symposium on Information Theory (ISIT)*. IEEE, 2019, pp. 1432–1436.
- [14] M. M. Amiri and D. Gunduz, “Federated learning over wireless fading channels,” *arXiv preprint arXiv:1907.09769*, 2019.
- [15] X. Cao, G. Zhu, J. Xu, and K. Huang, “Optimal power control for over-the-air computation in fading channels,” *arXiv preprint arXiv:1906.06858*, 2019.